

The ringing of quantum corrections Schwarzschild black hole with GUP*

Yujia Xing¹, Yi Yang¹, Dong Liu¹, Zheng-Wen Long^{1†} and Zhaoyi Xu^{1‡}

¹College of Physics, Guizhou University, Guiyang, 550025, China

April 26, 2022

Abstract

Schwarzschild black holes with quantum corrections are studied under scalar field perturbations and electromagnetic field perturbations to analyze the effect of the correction term on the potential function and quasinormal mode (QNM). In classical general relativity, spacetime is continuous and there is no existence of the so-called minimal length. The introduction of the correction items of the generalized uncertainty principle (GUP), i.e., the parameter β , can change the singularity structure of the hole-degree gauge and may lead to discretization in time and space. We apply the sixth-order WKB method to approximate the QNM of Schwarzschild black holes with quantum corrections and perform numerical analysis to derive the results of the method. Also, we find that the effective potential and QNM in electromagnetic fields are larger than those in scalar fields.

Keywords: Quantum corrections, Black hole, Quasinormal mode, Generalized uncertainty principle

PACS: 04.70.Dy, 04.70.-s, 04.30.-w, 04.70.Bw

1. Introduction

Black holes are one of the most important predictions of Einstein's general theory of relativity, and in order to more fully understand the physical properties of black holes, physicists have constructed different black hole solutions [1,2]. The shadow of the M87 [3–5] massive black hole, surrounded by a crescent-shaped aperture, was first obtained by the Event Horizon Telescope. Therefore, the black hole at the heart of the M87 elliptical galaxy has also become a key object of observation and analysis for many physicists. The LIGO-VIRGO collaboration [6–9] has successfully detected gravitational waves from the combination of a black hole and a neutron star, and this discovery is extremely important for the study of black holes, in other words through the observation of gravitational waves we can fully understand the nature of the event horizon of black holes. Gravitational waves from some dense objects produce echoes [10–20] during propagation, which makes the echoes inseparably linked to the unique properties of dense objects, and one uses this signal to analyze the inherent properties of dense

*Project supported by the National Natural Science Foundation of China (Grant Nos. 11465006, Grant Nos.11565009) and the Special Research Fund for Natural Science of Guizhou University (Grant No. X2020068).

[†]Corresponding author. E-mail:zwlong@gzu.edu.cn

[‡]Corresponding author. E-mail:zyxu@gzu.edu.cn

objects. It is also possible to observe gravitational wave echoes through the later stages of the QNM ringing.

Chandrasekhar [24] made a prominent contribution to the QNM in black holes, especially the effect of the QNM on the external perturbation of the black hole, the essence of which is that there is a QNM ringing at the late stage of the initial pulse for the outside of the black hole event horizon. QNM [25–37] is the vibrational frequency that is available at the pure outgoing wave at infinity and the pure incident wave in the event horizon with free vibration. QNM has been widely applied in recent years, including QNM in dark matter halos [38–40], QNM in charged black holes with electromagnetic field perturbations [41], QNM in the multi-dimensional Einstein-power-Maxwell case with scalar field perturbations in the spacetime context of black holes [42], perturbation studies of black holes to solve spectral related problems [43], the relationship between QNM and shading with quantum correcting [44], calculation of slow revolving black holes with dynamical Chern-Simons gravity using QNM [21], and the accurate solutions of Kerr black hole perturbations by using QNM [22,23].

The solution of a black hole has a singularity, i.e., there is a singularity that would cause general relativity to fail at that point. Therefore, physicists have made a lot of research to conclude that the GUP can be used to correct the black hole degree gauge [45–49], and have achieved important results. In 1968, Bardeen presented the regular black hole solutions [50]. In [51], Kazakov and Solodukhin used quantum correction terms to deform the Schwarzschild solution to avoid singularities. The QNM of the corrected Schwarzschild solution has been analyzed in [52]. In [53], electrons can be emitted across the potential barrier into the vacuum and thus quantum corrected Schwarzschild black holes embodying Hawking radiation. In view of the importance of the QNM to reflect the relevant properties near the apparent horizon of the black hole event, we will study the QNM of the black hole with GUP correction considered in this paper.

This paper is structured as follows. In Sec.2, we use the equations of the quantum-corrected metric in the presence of scalar and electromagnetic field perturbations to derive the corresponding effective potential bases and draw an image of the effective potential. In Sec.3, numerical calculation by WKB method to obtain the frequency of QNM. In Sec.4, the conclusions of this study were drawn.

2. The methods

2.1. Scalar and electromagnetic field perturbations in quantum-corrected Schwarzschild black hole

We use GUP to quantum correct the Schwarzschild black hole to analyze the QNM, as the Schwarzschild radius r_h is transformed into the GUP radius r_H [54], considering the GUP

$$\Delta x > \frac{\hbar}{\Delta p} + \left(\frac{\alpha l_{P1}^2}{\hbar}\right)\Delta p, \quad (1)$$

where α is positive dimensionless parameter, l_{P1} is the Planck length, $l_{P1} = \sqrt{\frac{\hbar G}{c^3}}$, and considering $\Delta x \rightarrow R$, $\Delta p \rightarrow cM$, then becomes

$$R > R'_C \equiv \frac{\hbar}{M_C} + \frac{\alpha GM}{c^2} = \frac{\hbar}{M_C} \left[1 + \alpha \left(\frac{M}{M_{P1}}\right)^2\right]. \quad (2)$$

GUP affects the size of the black hole horizon, then Eq.(2) is written as

$$R > R'_S = \frac{\alpha GM}{c^2} \left[1 + \frac{1}{\alpha} \left(\frac{M_{P1}}{M} \right)^2 \right]. \quad (3)$$

The free constant of Eq.(2) is related to the first term, then Eq.(2) and (3) are written as

$$R'_C = \frac{\beta \hbar}{M_C} \left[1 + \frac{2}{\beta} \left(\frac{M}{M_{P1}} \right)^2 \right] \quad (4)$$

and

$$R'_S = \frac{2GM}{c^2} \left[1 + \frac{\beta}{2} \left(\frac{M_{P1}}{M} \right)^2 \right] \quad (5)$$

where β is postive dimentionless parameter, $\hbar = c = G = 1$.

The corrected Schwarzschild black hole:

$$ds^2 = f(r)dt^2 - \frac{1}{f(r)}dr^2 - r^2(d\theta^2 + \sin^2 \theta d\phi^2), \quad (6)$$

where

$$f(r) = 1 - \frac{2}{M_{P1}^2} \frac{M}{r} \left(1 + \frac{\beta}{2} \frac{M_{P1}^2}{M^2} \right), \quad (7)$$

and r_H is written as

$$r_H = \frac{2}{M_{P1}^2} \left(\frac{M^2 + \frac{\beta}{2} M_{P1}^2}{M} \right) = R'_S, \quad (8)$$

with Schwarzschild black hole horizon $r_h=2M$.

In this study, we focus on the analysis of spacetime in the context of Schwarzschild black holes after quantum corrections in scalar and electromagnetic fields. Then the radial equation and the effective potential are derived.

For the massless scalar field :

$$\frac{1}{\sqrt{-g}} \partial_\mu (\sqrt{-g} g^{\mu\nu} \partial_\nu \Phi) = 0. \quad (9)$$

For the electromagnetic field equation :

$$\frac{1}{\sqrt{-g}} \partial_\nu (F_{\rho\sigma} g^{\rho\mu} g^{\sigma\nu} \sqrt{-g}) = 0, \quad (10)$$

where $F_{\rho\sigma} = \partial_\rho A_\sigma - \partial_\sigma A_\rho$, A_ν is an electromagnetic four-potential.

The tortoise coordinate is expressed as:

$$dr_* = \frac{dr}{f(r)}. \quad (11)$$

By splitting the variances Eqs.(9) and (10), the equation typically takes the Schrodinger form:

$$-\frac{d^2 \Psi}{dr_*^2} + V(r) \Psi = \omega^2 \Psi. \quad (12)$$

The effective potentials under the scalar and electromagnetic fields :

$$V_{\text{eff}} = \frac{f(r)}{r} \frac{df(r)}{dr} + \frac{f(r)l(l+1)}{r^2}, \quad (13)$$

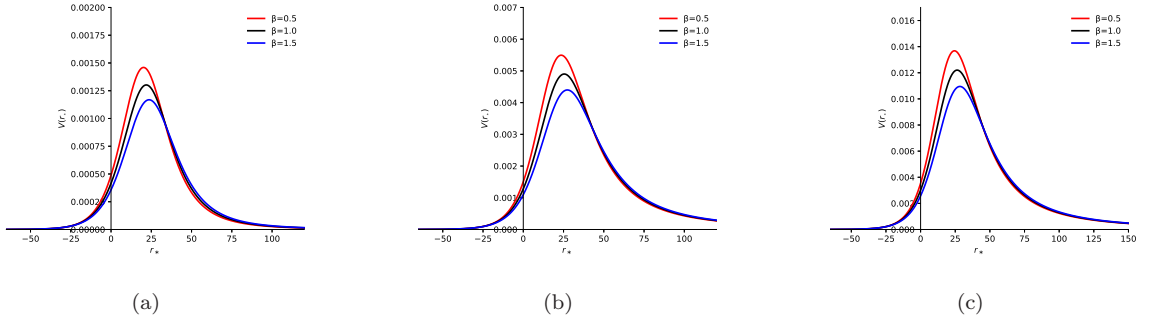


Figure 1: The effective potentials of the scalar field with the different l . (a) $l = 0$ (b) $l = 1$ (c) $l = 2$.

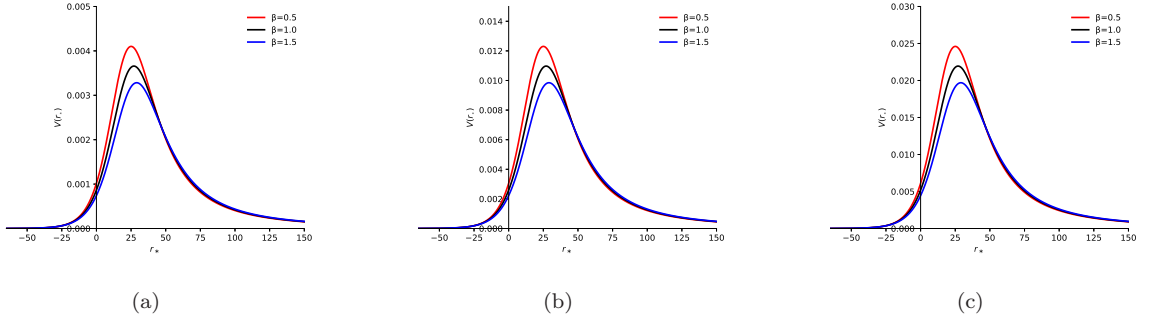


Figure 2: The effective potentials of the electromagnetic field with the different l . (a) $l = 1$ (b) $l = 2$ (c) $l = 3$.

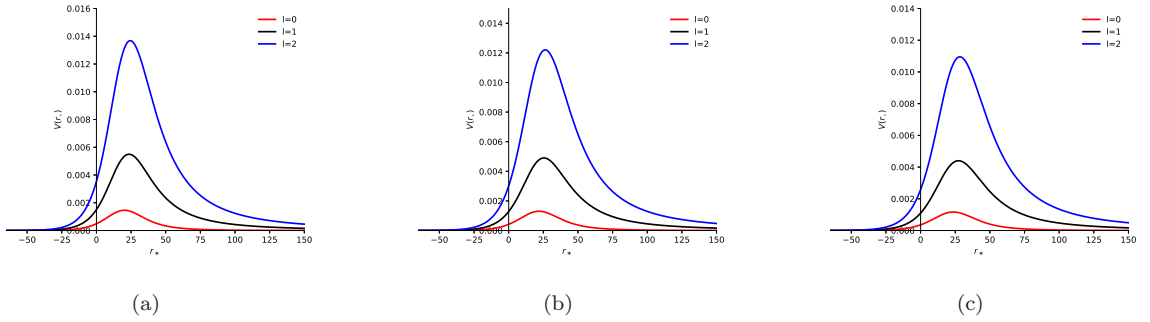


Figure 3: The effective potentials of the scalar field with the different β . (a) $\beta = 0.5$ (b) $\beta = 1.0$ (c) $\beta = 1.5$.

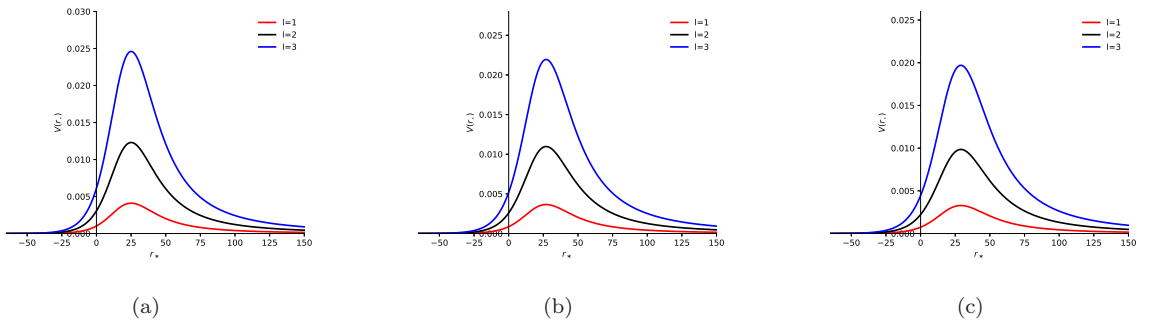


Figure 4: The effective potentials of the electromagnetic field with the different β . (a) $\beta = 0.5$ (b) $\beta = 1.0$ (c) $\beta = 1.5$.

$$V_{\text{em}} = \frac{f(r)l(l+1)}{r^2}. \quad (14)$$

Figs.1-4 show the effective potential for various parameters l and β . Figs.1-2 show that under the scalar and electromagnetic fields, when l is constant, the effective potential decreases with the increase of β , decays at infinity, and finally disappears, and then the black hole will return to the equilibrium state. Figs.3-4 show that when β is constant, the effective potential increases as l increases, and when r_* tends to infinity the effective potential approaches 0. The effective potential of the electromagnetic field under the same conditions is more than that of the scalar field.

2.2. The WKB method

The WKB method was firstly introduced by Schutz and Will [25] and then further explained by Konoplya [26–28]. We use the WKB method to study frequencies, the main idea of which is to expand the WKB series in the asymptotic region and to match the solution of this expanding at infinity with the Taylor unfolding around the effective potential peak. In this session, we study the QNM frequencies by means of the sixth-order WKB formula of the shape given below:

$$\frac{i(\omega^2 - V_0)}{\sqrt{-2V_0''}} - \sum_{i=2}^6 \Omega_i = n + \frac{1}{2}, \quad (15)$$

where V_0 is the maximal value of the effective potential at r_0 , V_0'' is the second order of the derivatives of the tortoise coordinates, Ω_i are the correction terms. we can obtain the point r_0 .

2.3. The time domain method

The time-domain integration method proposed by Gundlach, Price and Pullin [55,56] to study the process of change of dynamical equations. We use this method to calculate the variation of frequency with time in the background spacetime of the black hole. By introducing the light cone coordinates for numerical computation

$$\begin{aligned} u &= t - r_*, \\ v &= t + r_*, \end{aligned} \quad (16)$$

where u and v are integration constants, r_* is tortoise coordinate. The wave function equation is being given as

$$-4 \frac{\partial^2 \psi(\mu, \nu)}{\partial \mu \partial \nu} = V(\mu, \nu) \psi(\mu, \nu). \quad (17)$$

The effective potential is influenced by the light cone variable (16). The difference step of the discretization is shown in [56], this discretization scheme is given by

$$\Psi(N) = \Psi(W) + \Psi(E) - \Psi(S) - h^2 \frac{V(W)\Psi(W) + V(E)\Psi(E)}{8} + O(h^4). \quad (18)$$

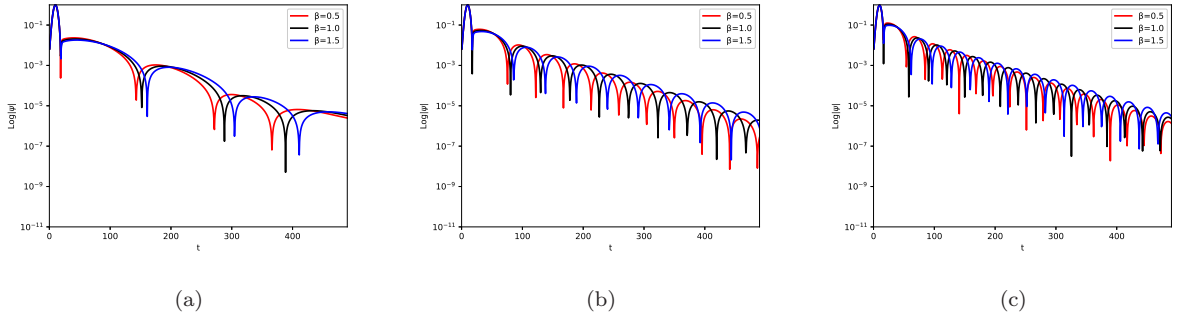
Where we use the following specified points $N = (u+h, v+h)$, $W = (u+h, v)$, $E = (u, v+h)$ and $S = (u, v)$, where $\nu = \nu_0$, $\mu = \mu_0$ are the initial datas. In order to contain the accuracy of the frequency analysis, we can control the parameters of the mathematical combination, adjust the differential grid and accuracy [57].

Table 1: The QNM frequencies of scalar field.

WKB method				
β	$l = 0$	$l = 1$	$l = 2$	$l = 3$
0.25	0.026779 - 0.024441 <i>i</i>	0.071008 - 0.023699 <i>i</i>	0.117247 - 0.023458 <i>i</i>	0.163725 - 0.023394 <i>i</i>
0.50	0.025991 - 0.023722 <i>i</i>	0.068919 - 0.023002 <i>i</i>	0.113798 - 0.022768 <i>i</i>	0.158910 - 0.022706 <i>i</i>
0.75	0.025248 - 0.023044 <i>i</i>	0.066950 - 0.022345 <i>i</i>	0.110547 - 0.022118 <i>i</i>	0.154369 - 0.022057 <i>i</i>
1.00	0.024547 - 0.022404 <i>i</i>	0.065091 - 0.021724 <i>i</i>	0.107476 - 0.021503 <i>i</i>	0.150081 - 0.021444 <i>i</i>
1.25	0.023885 - 0.021797 <i>i</i>	0.063331 - 0.021130 <i>i</i>	0.104571 - 0.020922 <i>i</i>	0.146025 - 0.020865 <i>i</i>
1.50	0.023255 - 0.021224 <i>i</i>	0.061665 - 0.020581 <i>i</i>	0.101819 - 0.020371 <i>i</i>	0.142182 - 0.020315 <i>i</i>

Table 2: The QNM frequencies of electromagnetic field.

WKB method				
β	$l = 1$	$l = 2$	$l = 3$	$l = 4$
0.25	0.0601676 - 0.022457 <i>i</i>	0.110932 - 0.023033 <i>i</i>	0.159248 - 0.023179 <i>i</i>	0.206811 - 0.023238 <i>i</i>
0.50	0.058398 - 0.021796 <i>i</i>	0.107669 - 0.022355 <i>i</i>	0.154564 - 0.022498 <i>i</i>	0.200728 - 0.022555 <i>i</i>
0.75	0.0567295 - 0.021174 <i>i</i>	0.104593 - 0.021716 <i>i</i>	0.150148 - 0.021855 <i>i</i>	0.194993 - 0.021910 <i>i</i>
1.00	0.055153 - 0.020586 <i>i</i>	0.101687 - 0.021113 <i>i</i>	0.145977 - 0.021248 <i>i</i>	0.189577 - 0.021302 <i>i</i>
1.25	0.053663 - 0.020029 <i>i</i>	0.098939 - 0.020541 <i>i</i>	0.142032 - 0.020674 <i>i</i>	0.184453 - 0.020726 <i>i</i>
1.50	0.052250 - 0.019502 <i>i</i>	0.096335 - 0.020002 <i>i</i>	0.138294 - 0.020129 <i>i</i>	0.179599 - 0.020181 <i>i</i>


 Figure 5: The dynamical evolutions of the scalar field with the different l . (a) $l = 0$ (b) $l = 1$ (c) $l = 2$.

3. Quantum-corrected Schwarzschild black hole model

In this session, we discuss the variation law of QNM for scalar and electromagnetic fields. To obtain the law we analyze the GUP corrected Schwarzschild black hole degree gauge, where the solution to Eq.(17) reflects the evolution process of the QNM. We respectively take $M = 1, M_{P1} = 0.5$, the different parameters of l and β , and then find the QNM variation law. We know that the variation law of the QNM for the modified Schwarzschild black hole is related to the effective potential. Since we want to quantitatively analyze this qualitative action, we have worked out the QNM frequencies via the sixth-order WKB method in the presence

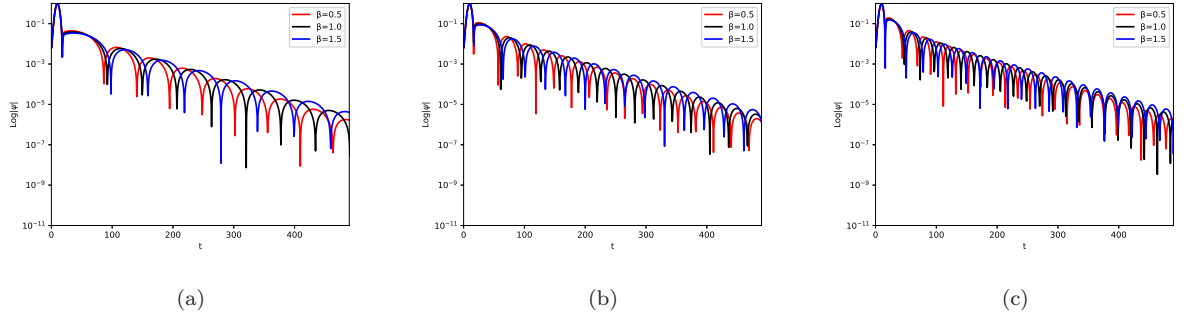


Figure 6: The dynamical evolutions of the electromagnetic field with the different l . (a) $l = 1$ (b) $l = 2$ (c) $l = 3$.

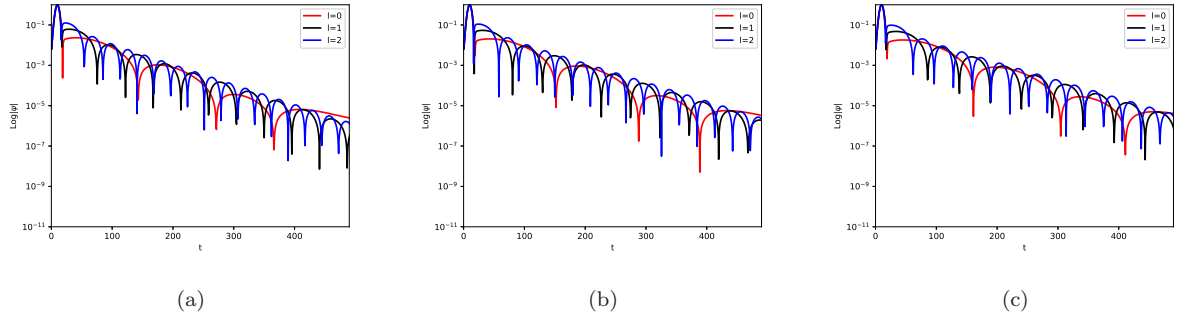


Figure 7: The dynamical evolutions of the scalar field with the different β . (a) $\beta = 0.5$ (b) $\beta = 1.0$ (c) $\beta = 1.5$.

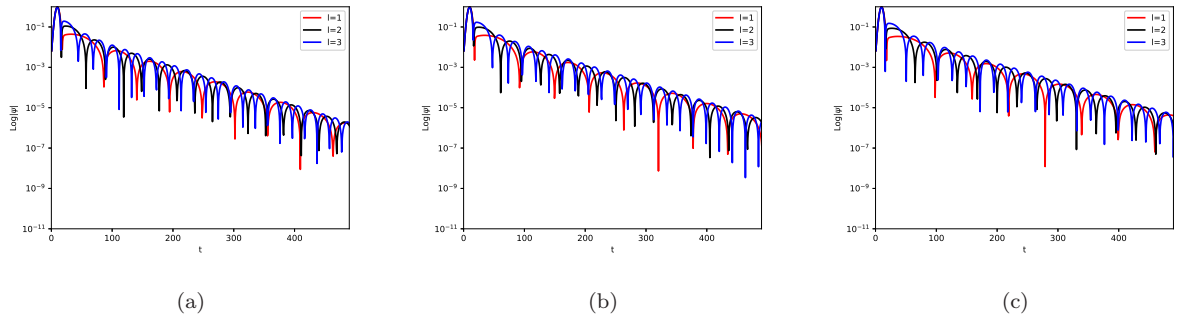


Figure 8: The dynamical evolutions of the electromagnetic field with the different β . (a) $\beta = 0.5$ (b) $\beta = 1.0$ (c) $\beta = 1.5$.

of scalar and electromagnetic fields. According to Tables 1-2, it can be seen that the corrected Schwarzschild black hole returns to steady state after a period of perturbation because the real part of the frequency is positive and the imaginary part is negative. As l is the same, the real imaginary parts of QNMs are decreasing as β increases, i.e., the oscillation frequency and damping rate are decreasing, and the more β the slower the decay. In the scalar field, when β is the same, as l increases, the real part of QNM increases and the imaginary part decreases. With larger l , the real part grows more rapidly and the imaginary part decays more slowly. In the electromagnetic field, the real and imaginary parts of the QNM increase as l increases. In a physical sense, the introduction of the parameter β can transform the singularity construction of the black hole metric since there are singularities in the solution of the black hole, i.e., singularities exist. This new GUP of correction items

may contribute to the discretization in time and space.

As can be seen from Figs.5-6, for l to be a constant value, the period of the QNM perturbation time is the shortest when $\beta = 0.5$, followed by $\beta = 1.0$ and the longest period of the QNM perturbation when $\beta = 1.5$. In Figs.7, it can be seen that when β is a fixed value, the period of the perturbation time of QNM is the least when l is much larger, and the magnitude of its period time is $l = 0 > l = 1 > l = 2$. Similarly, in Figs.8, the magnitude of the cycle time of the perturbation time of QNM is $l = 1 > l = 2 > l = 3$. The average value of the ringing of the QNM in the scalar and electromagnetic fields is about 10^{-1} and 10^{-8} . We can observe that the perturbation process in Fig.5(a) is clearly different from Fig.5(b) and Fig.5(c), due to the fact that the parameter l affects the frequency of the QNM.

4. Conclusions

In the present work, we study the QNM of the Schwarzschild black hole corrected by the GUP. We analyze the equations in scalar and electromagnetic fields and obtain the effective potential which corresponds to them. The calculation is performed by the sixth-order WKB method, which gives the frequency of the QNM. We mainly obtained the following results:

(1)The effective potential of the GUP quantum-corrected Schwarzschild black hole decrease with the increase of β , and increase with the increase of l . When r_* approaches infinity, the effective potential tends to 0 and the black hole will be unaffected by the change of parameters and finally comes back to the equilibrium state.

(2)The QNM ringing of the GUP quantum-corrected Schwarzschild black hole appears after the initial pulse. When l is fixed, the QNM oscillation becomes weaker as β increases, i.e., the correction term of GUP makes the black hole metric gauge not singular; when β is fixed, the QNM oscillation becomes stronger as l increases. It can be concluded that the trend of QNM is related to the effective potential.

(3)The QNM is a special characteristic of the solution of the black hole perturbation equation, which occupies the main time in the black hole perturbation process. The parameter l influences the perturbation time of QNM, among the most obvious in Fig.5(a), which affects the spacetime with black hole background. In other words, it affects the intrinsic frequency as well as the damping rate of the oscillation and is not affected by the initial oscillation.

(4)In Figs.5-6, when l is a constant value, the period of the time of QNM perturbation is $\beta = 1.5 > \beta = 1.0 > \beta = 0.5$, then $\beta = 0.5$ is easier to detect. In Fig.7, it is known that whenever β is a constant value, the duration of the perturbation time is $l = 0 > l = 1 > l = 2$, then $l = 2$ is more easily to be detected. In Fig.8, it is well recognized that as long as β is a constant, the length of the perturbation time is $l = 1 > l = 2 > l = 3$, then $l = 3$ is easy to be found.

(5)The average value of the ringing of QNM in scalar and electromagnetic fields is about in the range of 10^{-1} and 10^{-8} , which is in agreement with our results in Tables 1-2 .

(6)The QNM ringing of the electromagneticfield is larger than that of the scalar field, which means that the radiation excited by the perturbation in the electromagnetic field may be larger than that excited by the scalar field.

In the present work, we have taken into account the scalar and electromagnetic field perturbations, and it is known that the QNM signals of both perturbations have very close physical effects in the vicinity of the

black hole horizon. It is of significance that the gravitational field perturbation is also very interesting, and according to the study [58–61], the QNM signal can also be produced under gravitational perturbation. More gravitational radiation is produced under the gravitational field than under the outfield perturbation. Similarly we think it is also an interesting topic to consider quantum corrections below Schwarzschild black holes under gravitational fields.

References

- [1] Arias P J, Bargue P, Contreras E and Fuenmayor E 2022 *Astronomy* **1** 2-14
- [2] Dymnikova I , Dobosz A and So Bitysek 2022 *Universe* **8** 2 65
- [3] Akiyama K *et al.* [Event Horizon Telescope], 2019 *Astrophys. J. Lett.* **875** 1 L1
- [4] Akiyama K *et al.* [Event Horizon Telescope], 2019 *Astrophys. J. Lett.* **875** 1 L2
- [5] Akiyama K *et al.* [Event Horizon Telescope], 2019 *Astrophys. J. Lett.* **875** 1 L3
- [6] Abbott B P *et al.* [LIGO Scientific and Virgo], 2016 *Astrophys. J. Lett.* **818** 2 L22
- [7] Abbott B P *et al.* [LIGO Scientific and Virgo], 2016 *Phys. Rev. Lett.* **116** 6 061102
- [8] Abbott B P *et al.* [LIGO Scientific and Virgo], 2016 *Phys. Rev. X* **6** 4, 041015
- [9] Abbott B P *et al.* [LIGO Scientific and VIRGO], 2017 *Phys. Rev. Lett.* **118** 22 221101
- [10] Yang Y, Liu D , Xu Z, Xing Y, Wu S and Long Z W 2021 *Phys. Rev. D* **104** 10 104021
- [11] Churilova M S and Stuchlik Z 2020 *Class. Quant. Grav.* **37** 7 075014
- [12] Bronnikov K A and Konoplya R A 2020 *Phys. Rev. D* **101** 6 064004
- [13] Wang Y T, Li Z P , Zhang J, Zhou S Y and Piao Y S 2018 *Eur. Phys. J. C* **78** 482
- [14] Testa A and Pani P 2018 *Phys. Rev. D* **98** 044018
- [15] Cardoso V and Pani P 2017 *Nature Astron* **1** 586
- [16] Konoplya R A, Stuchl Z ík and Zhidenko A 2019 *Phys. Rev. D* **99** 024007
- [17] Ezquiaga J M, Hu W, Lagos M and Lin M X 2021 *JCAP* **11** 11 048
- [18] Cardoso V, Foit V F and Kleban M 2019 *JCAP* **08** 006
- [19] Chesler P M, Blackburn L, Doeleman S S, Johnson M D, Moran J M, Narayan R and Wielgus M 2021 *Class. Quant. Grav.* **38** 12 125006
- [20] Cadonati L, 2010 *J. Phys. Conf. Ser.* **222** 012030
- [21] Srivastava M, Chen Y and Shankaranarayanan S 2021 *Phys. Rev. D* **104**, 6, 064034
- [22] Bonelli G, Iossa C, Lichtig D P and Tanzini A 2022 *Phys. Rev. D* **105** 4 044047
- [23] Carullo G, Laghi D, Johnson-McDaniel N K, Del Pozzo W, Dias O J C, Godazgar M and Santos J E, 2022 *Phys. Rev. D* **105** 6 062009
- [24] Chandrasekhar S 1983 *The Mathematical Theory of Black Holes* (Oxford: Clarendon)
- [25] Schutz B F and Will C M 1985 *Astrophys. J. Lett.* **291** L33-L36
- [26] Iyer S and Will C M 1987 *Phys. Rev. D* **35** 3621
- [27] Iyer S 1987 *Phys. Rev. D* **35** 3632
- [28] Konoplya R A 2003 *Phys. Rev. D* **68** 024018
- [29] Bezares M, Bošković M, Liebling S. , Palenzuela C, Pani P and Barausse E 2022 *Phys. Rev. D* **105** 6 064067
- [30] Vieira H S, Destounis K and Kokkotas K D 2022 *Phys. Rev. D* **105** 4 045015
- [31] Fernandes T V, Hilditch D, Lemos J P S and Cardoso V 2022 *Phys. Rev. D* **105** 4 044017
- [32] Cano P A, Fransen K, Hertog T and Maenaut S 2022 *Phys. Rev. D* **105** 2 024064
- [33] Cadoni M, Oi M and Sanna A P 2021 *Phys. Rev. D* **104** 12, L121502
- [34] Mondkar S, Mukhopadhyay A, Rebhan A and Soloviev A 2021 *JHEP* **11**, 080
- [35] Destounis K, Macedo R P, Berti E, Cardoso V and Jaramillo J L 2021 *Phys. Rev. D* **104** 8 084091
- [36] Srivastava M, Chen Y and Shankaranarayanan S 2021 *Phys. Rev. D* **104** 6 064034

- [37] Cai X C and Miao Y G 2021 *Phys. Rev. D* **103** 12, 124050
- [38] Liu D, Yang Y, Wu S, Xing Y, Xu Z and Long Z W 2021 *Phys. Rev. D* **104** 10 104042
- [39] Zhang C, Zhu T and Wang A 2021 *Phys. Rev. D* **104** 12 124082
- [40] Barausse E, Cardoso V and Pani P, 2014 *Phys. Rev. D* **89** 10 104059
- [41] Nomura K and Yoshida D 2022 *Phys. Rev. D* **105** 4 044006
- [42] Liu Y and Jing J L 2012 *Chin. Phys. Lett.* **29** 010402
- [43] Hatsuda Y and Kimura M 2021 *Universe* **7** 12 476
- [44] Okyay M and Övgün A 2022 *JCAP* **01** 01 009
- [45] Anacleto M A, Campos J A V , Brito F A and Passos E 2021 *Annals Phys.* **434** 168662
- [46] Anacleto M A, Brito F A, Luna G C and Passos E 2022 *Annals Phys.* **440** 168837
- [47] Anacleto M A, Brito F A, Garcia C V, Luna G C and Passos E 2019 *Phys. Rev. D* **100** 10 105005
- [48] Sakalli I, Övgün A and Jusufi K 2016 *Astrophys. Space Sci.* **361** 10 330
- [49] Maluf R V and Neves J C S 2018 *Phys. Rev. D* **97** 10 104015
- [50] Bardeen J M 1968 Non-singular general relativistic gravitational collapse in Proc. Int. Conf. GR5 (Tbilisi, Georgia, USSR,) p. 174.
- [51] Kazakov D I and Solodukhin S N 1994 *Nucl. Phys. B* **429** 153-176
- [52] Konoplya R A 2020 *Phys. Lett. B* **804** 135363
- [53] Hajebrahimi M and Nozari K 2020 *PTEP* **2020** 4 043E03
- [54] Carr B J, Mureika J and Nicolini P 2015 *JHEP* **07** 052
- [55] Gundlach C., Price R H and Pullin J 1994 *Phys. Rev. D* **49** 883-889
- [56] Gundlach C, Price R H and Pullin J 1994 *Phys. Rev. D* **49** 890-899
- [57] Moderski R and Rogatko M 2005 *Phys. Rev. D* **72** 044027
- [58] Dong R. and Stojkovic D 2021 *Phys. Rev. D* **103** 024058
- [59] Dey R, Chakraborty S and Afshordi N 2020 *Phys. Rev. D* **101** 104014
- [60] Dey R, Biswas S and Chakraborty S 2021 *Phys. Rev. D* **103** 084019
- [61] Oshita N, Tsuna D and Afshordi N 2020 *Phys. Rev. D* **102** 024045